the FEBS Journal

The calcium transporter Pmc1 provides Ca^{2+} tolerance and influences the progression of murine cryptococcal infection

Livia Kmetzsch[1], Charley C. Staats[1], Julia B. Cupertino[1], Fernanda L. Fonseca[2], Marcio L. Rodrigues[2,3], Augusto Schrank[1] and Marilene H. Vainstein[1]

1 Centro de Biotecnologia, Universidade Federal do Rio Grande do Sul, Brazil
2 Instituto de Microbiologia Paulo de Góes, Universidade Federal do Rio de Janeiro, Brazil
3 Fundação Oswaldo Cruz – Fiocruz, Centro de Desenvolvimento Tecnológico em Saúde (CDTS), Rio de Janeiro, Brazil

Keywords
calcium transport; cryptococcosis; *Cryptococcus neoformans*; vacuolar calcium storage; virulence

Correspondence
M. H. Vainstein, Centro de Biotecnologia, Universidade Federal do Rio Grande do Sul, Av. Bento Gonçalves 9500, 43421, Caixa Postal 15005, Porto Alegre, RS 91501-970, Brazil
Fax: +55 51 3308 7309
Tel: +55 51 3308 6060
E-mail: mhv@cbiot.ufrgs.br

(Received 12 June 2013, revised 15 July 2013, accepted 26 July 2013)

doi:10.1111/febs.12458

The Ca^{2+}-calcineurin signaling pathway in the human fungal pathogen *Cryptococcus neoformans* is essential for adaptation to the host environment during infection. Calcium transporters regulate cytosolic calcium concentrations, providing Ca^{2+} loading into storage organelles. The three calcium transporters that have been characterized in *C. neoformans*, Cch1, Eca1 and Vcx1, are required for fungal virulence, supporting a role for calcium-mediated signaling in cryptococcal pathogenesis. In the present study, we report the functional characterization of the putative vacuolar calcium ATPase Pmc1 in *C. neoformans*. Our results demonstrate that Pmc1 provides tolerance to high Ca^{2+} concentrations. The double knockout of *C. neoformans PMC1* and *VCX1* genes impaired the intracellular calcium transport, resulting in a significant increase in cytosolic calcium levels. Furthermore, Pmc1 was essential for both the progression of pulmonary infection and brain colonization in mice, emphasizing the crucial role of calcium signaling and transport for cryptococcal pathogenesis.

Introduction

In eukaryotic cells, ionic calcium (Ca^{2+}) is an intracellular regulator of a wide variety of signaling pathways. One of the key activities of intracellular Ca^{2+} involves the Ca^{2+} binding protein calmodulin, which activates the phosphatase calcineurin in response to increasing cytosolic calcium levels [1,2]. The Ca^{2+} levels are coordinated by transporters located in the plasma, vacuolar or endoplasmic reticulum (ER) membranes. Activated calcineurin mediates nuclear translocation of specific transcription factors, which trigger the expression of calcineurin-responsive genes [3,4]. These gene products allow the cell to cope with stress and maintain Ca^{2+} homeostasis. Ca^{2+} related pathways have been associated with crucial pathogenic processes in different fungal pathogens, including *Cryptococcus neoformans*, *Cryptococcus gattii*, *Candida albicans* and *Aspergillus fumigatus* [5–8].

The calcium-calcineurin signaling pathway in the human pathogenic fungus *C. neoformans* is essential for adaptation to the host milieu and establishment of infection [9]. Calcineurin is required for fundamental biological events of *C. neoformans*, such as mating, morphogenesis, growth at 37 °C and virulence [7,10–13]. Moreover, the *C. neoformans* transcription factor Crz1 is calcineurin activated and regulates cell wall integrity [14]. *C. neoformans* calmodulin is critical for

Abbreviations
CFU, colony forming unit; ER, endoplasmic reticulum; Fura-2 AM, Fura-2 acetoxymethylester; GXM, glucuronoxylomannan; WT, wild type; YPD, yeast extract–peptone–dextrose medium.

cell viability and for fungal response to high temperatures [15]. Other important components of the calcium-calcineurin signaling network in *C. neoformans* are the Ca^{2+} transporters Cch1, Eca1 and Vcx1. Cch1 mediates Ca^{2+} entry in fungal cells and is required for the uptake of this ion in low Ca^{2+} environments [16]. Eca1, a sarcoplasmic/endoplasmic reticulum Ca^{2+}-ATPase, participates in stress tolerance [17]. Vcx1, a vacuolar Ca^{2+}-exchanger, regulates Ca^{2+} tolerance [18]. Importantly, Cch1, Eca1 and Vcx1 are involved in *C. neoformans* virulence [16–18], demonstrating the importance of Ca^{2+}-mediated signaling in this pathogen.

Ca^{2+} transporters mediate the transfer of free ions from the cytosol to storage organelles, preventing toxicity. The vacuole is the major Ca^{2+} storage organelle in many eukaryotes, including fungi. In this organelle, Ca^{2+}-ATPases and Ca^{2+}exchangers facilitate the accumulation of Ca^{2+} (reviewed in [19]). In *Saccharomyces cerevisiae*, the Ca^{2+}-ATPase Pmc1 regulates cytosolic calcium levels, providing Ca^{2+} tolerance and vacuolar Ca^{2+} loading [19,20]. We previously demonstrated that the *PMC1* ortholog is upregulated in the *C. neoformans vcx1* knockout strain, possibly because Pmc1 also transports Ca^{2+} into vacuoles, generating functional redundancy [18]. Here, we report the functional characterization of the *C. neoformans PMC1* gene. For this purpose, a *pmc1* null mutant, a double *pmc1 vcx1* mutant and relevant complemented strains were constructed. The *PMC1* knockout resulted in hypersensitivity to high Ca^{2+} concentrations, a phenotype that was even more pronounced in the *pmc1 vcx1* double knockout strain. Furthermore, disruption of *PMC1* influenced the relative intracellular Ca^{2+} concentration. Notably, lack of Pmc1 interfered with *C. neoformans* virulence in mice.

Results

In silico characterization of the vacuolar Ca^{2+}-ATPase *PMC1* ortholog in *C. neoformans*

The *PMC1* gene was identified in the *C. neoformans* H99 genomic database at the Broad Institute (accession number CNAG_01232.2) based on its similarity to the vacuolar Ca^{2+}-ATPase from *S. cerevisiae*. The *C. neoformans PMC1* coding region is 4655 bp long, contains eight introns, and encodes a putative 1414-amino-acid protein. BLAST search using the Conserved Domain Database at NCBI revealed the presence of the following conserved domains in the *C. neoformans* Pmc1 ortholog: a cation ATPase C domain (PFAM00689), an E1–E2 ATPase domain (PFAM00122), a haloacid dehalogenase-like hydrolase domain (PFAM00702) and a cation transporter ATPase N domain (PFAM 00690). Additionally, phylogenetic analysis including Pmc1 sequences from distinct eukaryotic organisms revealed that the *C. neoformans* Pmc1 had the highest similarity to the *Ustilago maydis* Pmc1 ortholog (55% identity and 69% similarity; Fig. 1). Prediction of transmembrane regions revealed that *C. neoformans* Pmc1 has 10 transmembrane domains, which is in agreement with the properties of well-described Ca^{2+}-ATPases [19].

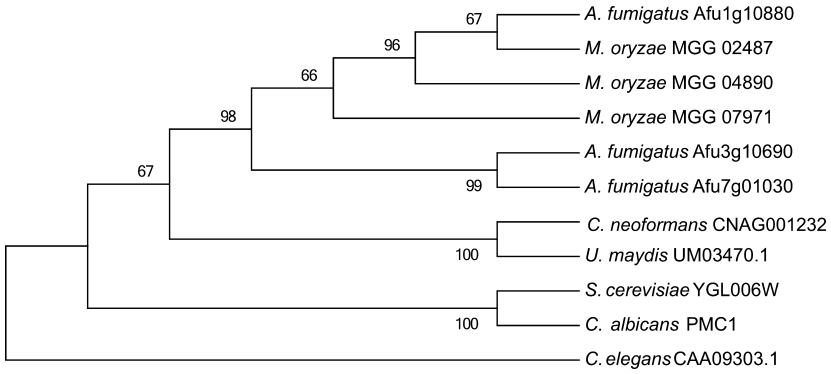

Fig. 1. Phylogenetic analysis of *C. neoformans* Pmc1 orthologs. The analysis was conducted by applying the neighbor-joining method and included Pmc1 sequences from distinct eukaryotic organisms (*S. cerevisiae*, *Saccharomyces* Genome Database accession number YGL006W; *C. albicans*, *Candida* Genome Database accession number orf 19.1727; *A. fumigatus*, *Aspergillus* Genome Database, accession numbers Afu1g10880 (PmcA), Afu3g10690 (PmcB), Afu7g01030 (PmcC); *U. maydis*, Broad Institute accession number UM_03470.1; *M. oryzae*, Broad Institute accession numbers MGG_07971, MGG_04890, MGG_02487; *C. elegans*, NCBI accession number CAA09303.1; *C. neoformans*, Broad Institute accession number CNAG_01232). The bar marker indicates genetic distance, which is proportional to the number of amino acid substitutions. Bootstrap values obtained from 1000 resamplings are shown at the nodes.

The *C. neoformans pmc1* mutant displayed sensitivity to high calcium concentrations

The Ca^{2+} calcineurin signaling network in *C. neoformans*, which is crucial for adaptation to the host [9], includes the vacuolar Ca^{2+} transporter Vcx1 [18]. *C. neoformans vcx1* mutant cells have an altered calcineurin-dependent Ca^{2+} tolerance and a reduced ability to kill mice [18]. On the basis of these observations, we asked whether Pmc1 is involved in similar events. For this purpose, a *pmc1* null mutant, a *pmc1 vcx1* double mutant and complemented strains were constructed (Fig. S1). The role of *C. neoformans* Pmc1 in Ca^{2+} tolerance was evaluated by monitoring the growth of the mutant strains on yeast extract–peptone–dextrose medium (YPD) agar plates supplemented with increasing concentrations of $CaCl_2$. The *pmc1* mutant strain had a reduced growth rate under high Ca^{2+} conditions (Fig. 2A). This phenotype was accentuated in the *pmc1 vcx1* double mutant, which manifested similar growth defects at lower Ca^{2+} concentrations. We also evaluated growth rates of the *C. neoformans pmc1* mutant strains in the presence of other divalent cations (Cd^{2+} and Mn^{2+}). In general, no significant differences in fungal growth were observed on agar plates containing 4 mM $MnCl_2$. The only exception was the *pmc1 vcx1* double mutant, which displayed impaired growth under these conditions. The *pmc1* and *pmc1 vcx1* mutant strains exhibited increased resistance to 50 μM $CdCl_2$ in comparison to wild-type (WT) and complemented strains (Fig. 2B).

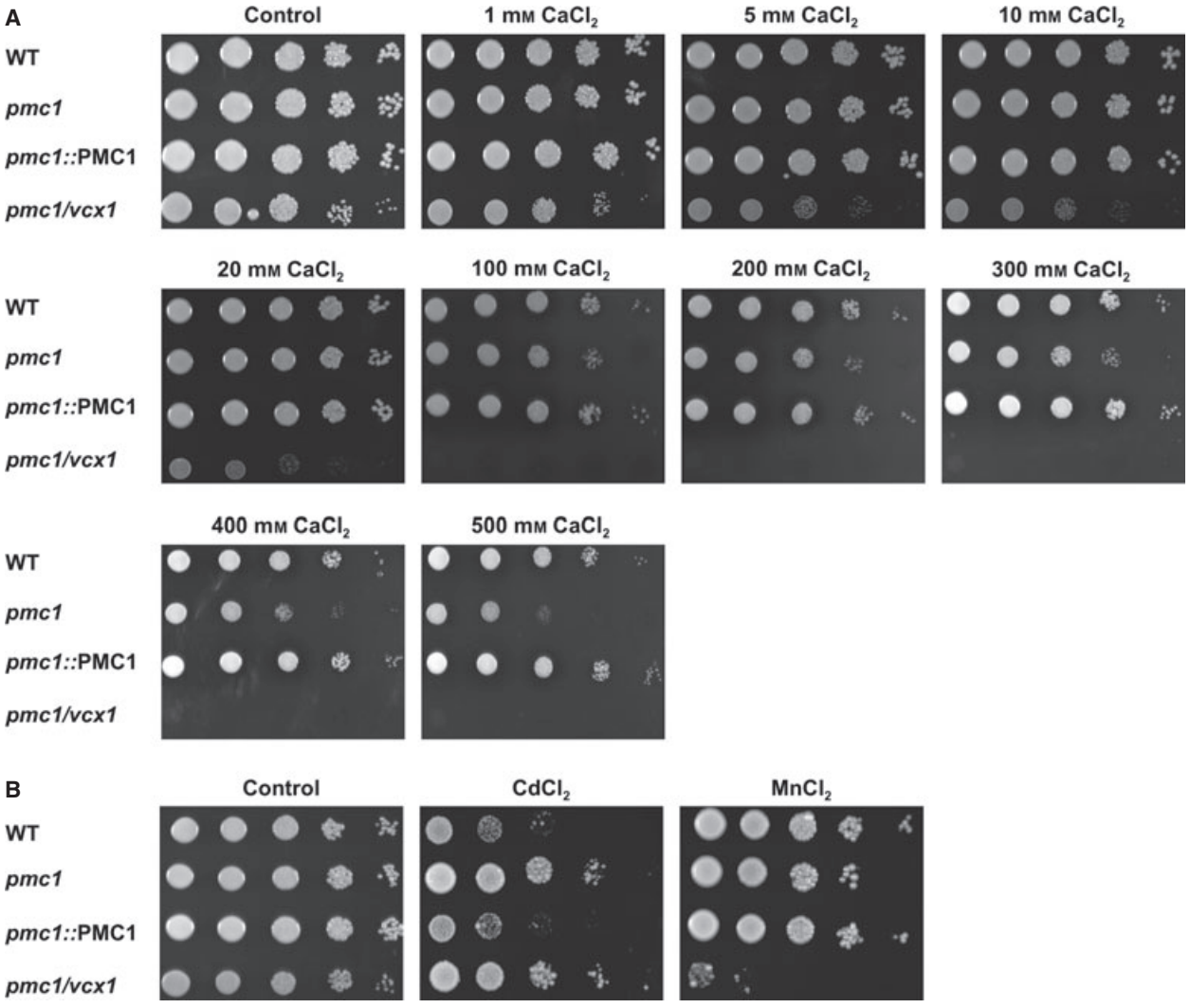

Fig. 2. *C. neoformans* Pmc1 is involved in Ca^{2+} tolerance. Ten-fold serial dilutions of WT, *pmc1* mutant, *pmc1 vcx1* mutant, *vcx1* mutant and *pmc1*::PMC1 complemented cell suspensions were plated onto YPD agar containing 1–500 mM $CaCl_2$ (A) or $MnCl_2$ or $CdCl_2$ (4 mM and 50 μM, respectively; B). The plates were incubated for 2 days at 30 °C. Control samples consisted of cells grown in YPD agar only.

Disruption of *PMC1* led to defective growth and impaired capsule formation in DMEM

Growth at 37 °C, capsule formation and melanin production were evaluated in the *pmc1* mutant strains because these attributes are determinants for *C. neoformans* virulence [21]. Disruption of *PMC1* did not interfere with melanin production or with the ability to grow at human body temperature. The only exception was the *pmc1 vcx1* double mutant, which displayed a slight growth defect at 37 °C (Fig. S2). Capsule formation and extracellular glucuronoxylomannan (GXM) release were affected in *pmc1* mutant strains under specific conditions. When the cells were incubated in DMEM, a medium that has been reported to induce capsule enlargement, capsule formation and extracellular GXM release were impaired (Fig. 3A). Apparently, this observation is associated with other alterations in the fungal physiology, since fungal growth was also reduced when the mutant strains were cultivated in DMEM (Fig. 3C). The *pmc1 vcx1* double mutant also showed a slightly increased sensitivity to 5% CO_2 *in vitro* (Fig. S3). These phenotypic attributes were not observed in mutant cells that were incubated in minimal medium, another classical capsule-inducing condition (Fig. 3B). Capsular polysaccharides produced by WT, *pmc1*, *pmc1 vcx1* and complemented cells were regularly recognized by monoclonal antibody 18B7 in both capsule-induction conditions, as demonstrated by immunofluorescence analysis (Fig. 3D).

Disruption of *PMC1* influences the relative level of intracellular calcium concentration in *C. neoformans* cells

The relative concentration of free intracellular Ca^{2+} in WT, *pmc1*, *pmc1 vcx1* and complemented strains was determined using the Ca^{2+}sensitive dye Fura-2 acetoxymethylester (Fura-2 AM) (Invitrogen, Carlsbad, CA, USA) [18]. The *pmc1* and *pmc1 vcx1* mutants had increased relative intracellular calcium concentrations compared with WT and complemented strains (Fig. 4). This difference was more pronounced in the *pmc1 vcx1* double mutant strain. These findings indicate that the loss of *PMC1* and *VCX1* could lead to a severe defect in intracellular calcium transport because both transporters regulate the cytosolic Ca^{2+} concentration and uptake into vacuoles [19].

Loss of *PMC1* affects the relative expression of other Ca^{2+} transporters in *C. neoformans*

Transcript levels of the Ca^{2+} calcineurin-related *CCH1*, *ECAI*, *VCX1* and *PMR1* Ca^{2+} transporters were evaluated in the WT, *pmc1*, *pmc1 vcx1* and *vcx1* mutant strains. Disruption of *PMC1* led to a decrease in the expression of *VCX1* and to an increase in the expression of *ECA1* after a 10 min exposure to 100 mM $CaCl_2$ ($P < 0.01$) (Fig. 5). However, *CCH1* and *PMR1* transcript levels were not significantly affected in the *pmc1* mutant strain. No statistically significant differences were observed in the transcript levels of calcium transporters in the control condition.

Pmc1 is required for the progression of murine cryptococcal infection

Since all the previously characterized calcium transporters modulate virulence in *C. neoformans* [16–18], we asked whether Pmc1 could also have a role in cryptococcal pathogenesis. Mice infected with WT or complemented strains had similar mean survival periods of 22 and 26 days, respectively ($P = 0.0053$). In contrast, *pmc1* and *pmc1 vcx1* mutant cells were strongly attenuated for virulence ($P < 0.0001$) (Fig. 6A). The fungal burden in the lungs and brain of animals infected with WT, *pmc1*, *pmc1 vcx1* and complemented strains was determined at 3, 7, 14 and 19 days post-infection. We found that *pmc1* mutant strains displayed greatly reduced fungal burdens in lung tissues at all days analyzed compared with WT and complemented strains, indicating that Pmc1 is important for the progression of pulmonary infection in mice (Fig. 6B). Importantly, no viable fungal cells were recovered from the lungs of mice infected with the *pmc1 vcx1* double mutant at days 14 and 19 post-infection, most probably due to

Fig. 3. The *C. neoformans pmc1* mutant presented growth defects and impaired capsule formation under specific growth conditions. (A) India ink counterstaining, capsule measurements and extracellular GXM determination in *C. neoformans* cultures incubated under capsule-inducing conditions (DMEM, 37 °C, 5% CO_2): $^{*}P < 0.05$; $^{****}P < 0.0001$. (B) India ink counterstaining, capsule measurements and extracellular GXM determination in *C. neoformans* cultures incubated in minimal medium at 30 °C. (C) Growth rates of WT, *pmc1* mutant, *pmc1 vcx1* mutant and complemented strains after incubation in DMEM: $^{*}P < 0.05$; $^{**}P < 0.01$ (24 h); $^{\#\#}P < 0.01$ (48 h). (D) Confocal microscopy of WT, *pmc1* mutant, *pmc1 vcx1* mutant and complemented cells incubated in DMEM or minimal medium (MM), as indicated. Cells were stained with calcofluor white (blue) and with the monoclonal antibody 18B7 (green) to visualize cell wall chitin and GXM, respectively. Bars, 5 μm.

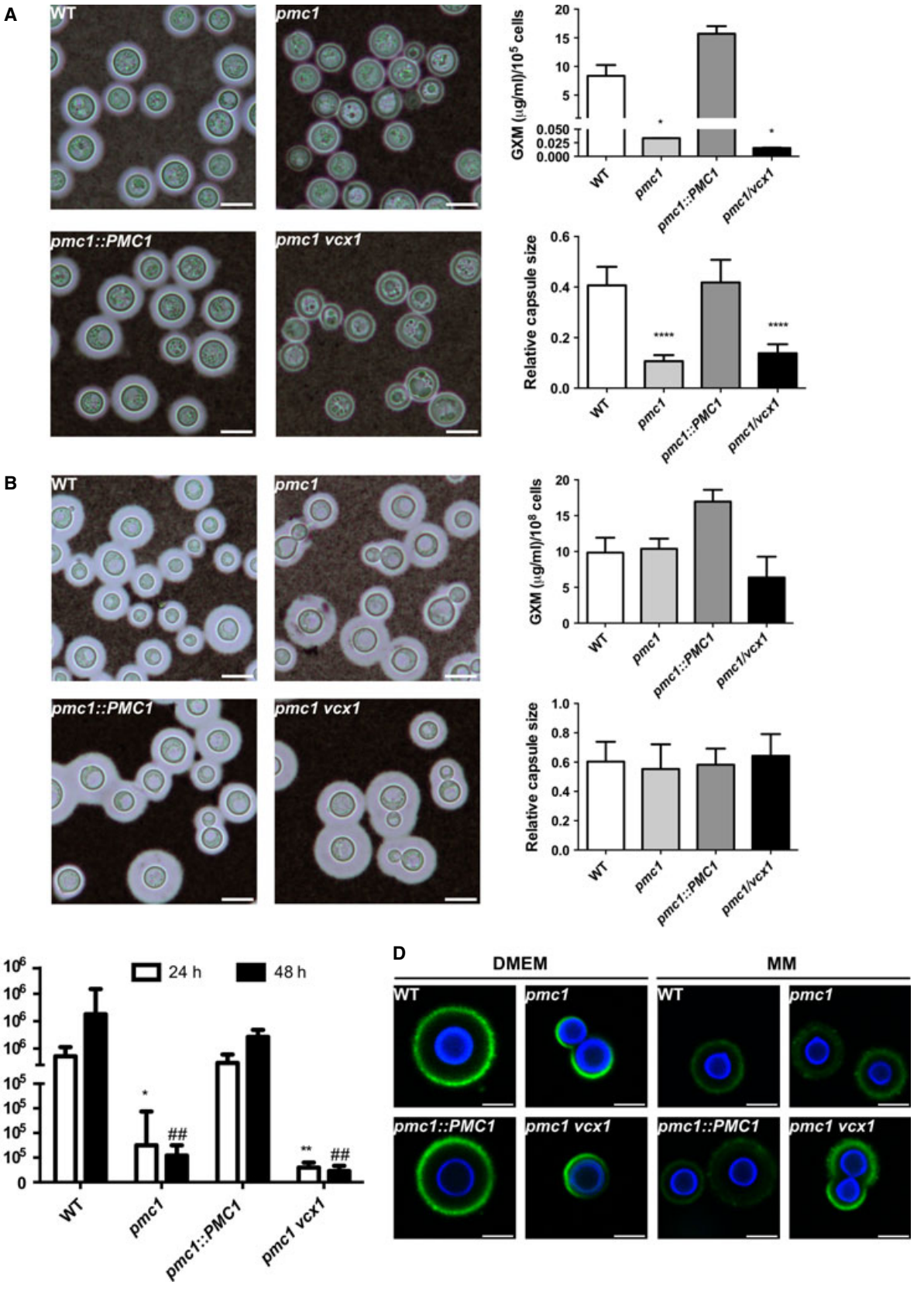
A
WT
pmc1
pmc1::PMC1
pmc1 vcx1
GXM (μg/ml)/10^5 cells
Relative capsule size
WT
pmc1
pmc1::PMC1
pmc1/vcx1
B
WT
pmc1
pmc1::PMC1
pmc1 vcx1
GXM (μg/ml)/10^8 cells
Relative capsule size
WT
pmc1
pmc1::PMC1
pmc1/vcx1
C
24 h
48 h
CFU.mL^-1
WT
pmc1
pmc1::PMC1
pmc1 vcx1
D
DMEM
MM
WT
pmc1
pmc1::PMC1
pmc1 vcx1

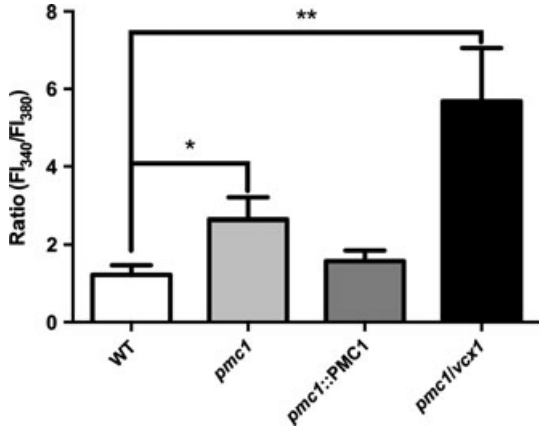

Fig. 4. Disruption of *PMC1* interferes with the relative intracellular Ca^{2+} levels in *C. neoformans*. The relative levels of intracellular Ca^{2+} in WT, *pmc1* mutant, *pmc1 vcx1* mutant and complemented cells were determined using Fura-2 AM. The relative Ca^{2+} concentration was determined based on the fluorescence ratio after dual-wavelength excitation. Data represent means ± standard deviations. $*P < 0.05$; $**P < 0.01$.

infection clearance. Furthermore, animals infected with the *pmc1* or *pmc1 vcx1* mutant strains had no fungal burden in brain tissues, in contrast to what was observed for WT and complemented strains. Together, these observations demonstrate that Pmc1 is critical for *C. neoformans* virulence in a mice model of cryptococcosis.

The hypocapsular phenotype observed after incubation of *pmc1* and *pmc1 vcx1* mutant cells in DMEM led us to ask whether these cells had the same phenotype during pulmonary infection. This question was addressed in supernatants of macerated lungs excised from mice infected with WT, *pmc1*, *pmc1 vcx1* or complemented strains at day 7 post-infection. India ink counterstaining of these cells revealed normal capsules, indicating proper capsular assembly by the *pmc1* mutant strains *in vivo* (Fig. 6C).

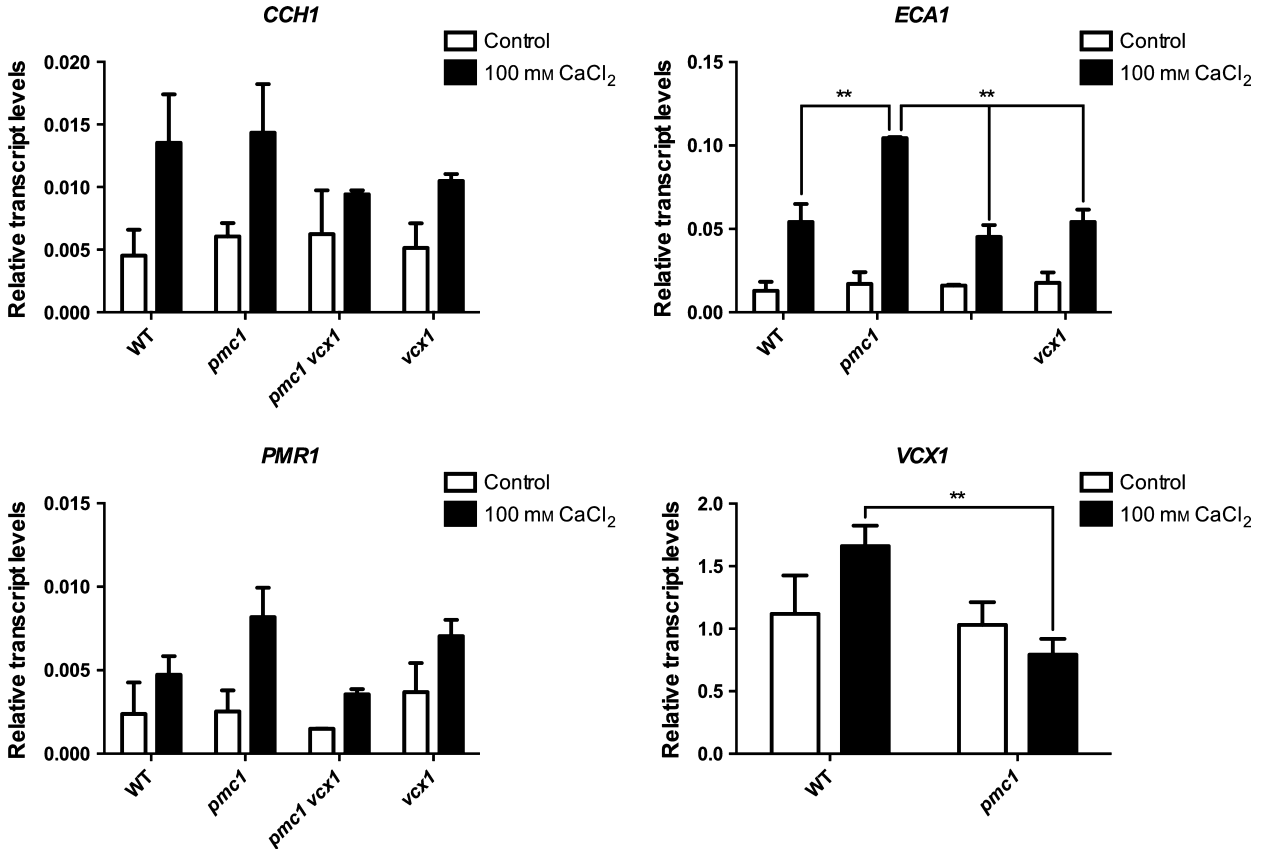

Fig. 5. Loss of *PMC1* affects the relative expression of other Ca^{2+} transporters after exposure to $CaCl_2$. The relative expression levels of various *C. neoformans* calcium transporters (*CCH1*, *ECA1*, *PMR1* and *PMC1*) in WT, *pmc1* mutant, *pmc1 vcx1* mutant and *vcx1* mutant cells were quantified by qRT-PCR. The data were normalized to actin cDNA levels in each set of PCR experiments. Data represent means ± standard deviations. $*P < 0.05$; $**P < 0.01$.

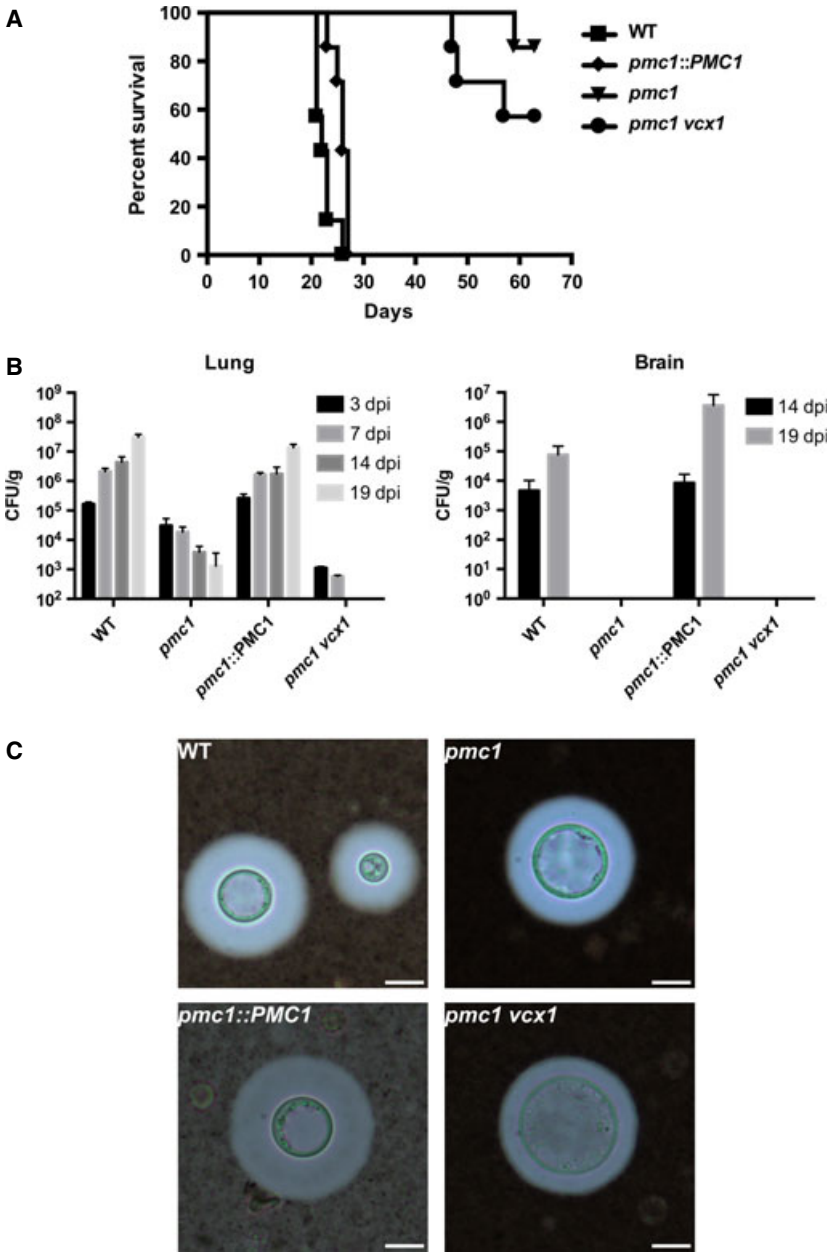

Fig. 6. Pmc1 is essential for cryptococcal pathogenesis in mice. Mortality curves (A) and fungal loads (B) of mice infected with WT, *pmc1* mutant, *pmc1 vcx1* mutant and *pmc1*::PMC1 strains. (C) India ink counterstaining of fungal cells recovered from infected lungs at day 7 post-infection. Bars, 10 μm.

Discussion

The Ca^{2+}-calcineurin signaling network is essential to many pathogenic mechanisms of *C. neoformans*, including mating, morphogenesis and growth at 37 °C [7,9,12,13]. In the present study, we characterized a new component of the Ca^{2+}-mediated signaling pathway in *C. neoformans*: the vacuolar Ca^{2+}-ATPase Pmc1. Fungal Ca^{2+}-ATPases are high affinity Ca^{2+} transporters that mediate the uptake of this ion into storage organelles in response to small alterations in cytosolic Ca^{2+} [19]. In particular, vacuolar Ca^{2+}ATPases play an important role in calcium tolerance, as concluded from the observation that the *PMC1* knockout in *S. cerevisiae* led to a Ca^{2+} hypersensitivity phenotype [20]. This observation corroborates our

findings that *C. neoformans* Pmc1 is involved in Ca^{2+} tolerance in the presence of high concentrations of $CaCl_2$. The vacuolar calcium exchanger Vcx1 partially contributes to this process, as inferred from the fact that the *C. neoformans pmc1 vcx1* double mutant exhibited high sensitivity to low concentrations of $CaCl_2$, indicating that vacuolar Ca^{2+} uptake is dramatically impaired in this mutant strain. Interestingly, a cadmium-resistance phenotype was detected for the *pmc1* and *pmc1 vcx1* mutant strains. Based on gene expression data, Mielniczki-Pereira *et al.* showed that *S. cerevisiae* Pmc1 could be involved in cadmium tolerance, but no significant sensitivity to Cd^{2+} was detected in *S. cerevisiae pmc1* cells [22].

Our assays aiming at the characterization of additional regulators of the physiology of Ca^{2+} distribution in *C. neoformans* efficiently illustrate the need for different experimental conditions for phenotypic analysis of fungal mutants. For instance, Pmc1 was required for fungal growth and capsule formation when *C. neoformans* was incubated in DMEM but not in minimal medium or *in vivo*. This observation strongly suggests that *PMC1* responds differently to specific conditions of the microenvironment to which the fungus is exposed. The components of DMEM that interfere with the physiological role of Pmc1 are still unknown. The ability to induce the formation of a polysaccharide capsule in response to a variety of host-specific environmental stimuli is one of the most important *C. neoformans* virulence attributes, which stimulates the investigation of this putative *PMC1* regulator. Capsule formation is a complex biological process that is regulated at multiple levels, including the biosynthesis of basic components, the transfer of glycosyl units, polysaccharide transport, and its assembly and maintenance at the cell surface (reviewed in [23]). Divergence in capsular phenotypes was also described for *C. neoformans rim20* and *rim101* mutant strains when cultured in distinct capsule-inducing media [24]. In addition, deletion of *GRASP*, the gene coding an essential regulator of polysaccharide secretion in *C. neoformans*, resulted in smaller capsules *in vitro*, but the mutant produced regular amounts of GXM during lung infection [25].

Cryptococcus neoformans Pmc1 also affected the expression of other calcium transporters. We previously demonstrated that *PMC1* is upregulated in the *vcx1* knockout strain, most probably due to a compensatory effect and functional redundancy [18]. However, in response to $CaCl_2$ exposure, we found that *VCX1* is downregulated in the *pmc1* knockout strain, indicating the existence of a complex system that regulates calcium transport in *C. neoformans*. In *S. cerevisiae*, calcineurin reduces the Ca^{2+} tolerance of *pmc1* mutants through inhibition of Vcx1 function [26]. This observation may be related to our current findings. Furthermore, there was an increase in *ECA1* expression in the *pmc1* mutant strain in response to a short time exposure to $CaCl_2$. Interestingly, *ECA1* expression was not affected by deletion of *VCX1* in the *pmc1* strain. A similar trend was observed when *PMR1* was analyzed, but the differences in relative expression levels were not statistically significant.

Our findings demonstrated that the vacuolar calcium transporter Pmc1 is required for *C. neoformans* virulence in a mouse model of cryptococcosis. Reduced proliferation of *pmc1* and *pmc1 vcx1* mutant cells in the murine host was observed, as concluded from the reduced fungal burden in lung tissues and impaired brain colonization. The molecular mechanisms involved in dissemination are not yet completely understood; however, there are a number of *C. neoformans* mutants that fail to cause central nervous system disease (reviewed in [27]). The genes deleted in these mutants are involved in a variety of cellular functions, suggesting that deletion of *PMC1* and *VCX1* cause general defects in fungal physiology and consequently altered survival during interaction with the host. The impaired virulence of the mutant strains described in this study could be related to a defect in vacuolar Ca^{2+} uptake, which would result in excessive cytosolic Ca^{2+} concentrations. This perturbation of Ca^{2+} homeostasis may interfere with a wide variety of signaling pathways involved in *C. neoformans* pathogenesis. Importantly, the *C. neoformans* calcium transporters Cch1, Eca1 and Vcx1 also modulate virulence [16–18], supporting a crucial role of Ca^{2+} transport in cryptococcal pathogenesis. The function of Pmc1 in fungal virulence has been reported in other human and plant pathogens, including *A. fumigatus* and *Magnaporthe oryzae* [28,29]. The *A. fumigatus pmcA* mutant strain also displayed calcium sensitivity and attenuated virulence [28]. The knockdown of three *M. oryzae PMC1* homologs resulted in significant reduction in mycelial melanization and conidial development. Additionally, the *M. oryzae PMC1* homologs were essential for pathogenicity in plant hosts [29]. These observations reinforce the essential role for Pmc1 in fungal pathogenesis.

In conclusion, we have shown that Pmc1, a vacuolar Ca^{2+}-ATPase, is required for essential cellular physiology and virulence events in *C. neoformans*. These events include Ca^{2+} tolerance, regulation of intracellular Ca^{2+} concentration and progression of cryptococcosis in mice. Although it is clear that further studies are required for a complete understanding of how Ca^{2+} homeostasis associated with virulence is regulated in *C. neoformans*, these results reveal previously

unknown aspects of the mechanisms by which the fungus controls Ca^{2+} availability. Our data also reinforce the notion that Ca^{2+} regulation is absolutely essential to the pathogenic processes required for the development of cryptococcosis.

Materials and methods

Fungal strains, plasmids and media

The *C. neoformans* serotype A strain H99 was utilized for the construction of the *pmc1* mutant strain. Fungal cells were maintained on YPD medium (1% yeast extract, 2% peptone, 2% dextrose and 1.5% agar). YPD plates containing nourseothricin (100 $\mu g \cdot mL^{-1}$) were used to select *C. neoformans PMC1* knockout transformants (*pmc1* and *pmc1 vcx1* strains). YPD plates supplemented with hygromycin (200 $\mu g \cdot mL^{-1}$) were used to select *C. neoformans PMC1* complementation transformants (*pmc1*::*PMC1* strain). The pJAF15 [30] and pAI4 [31] plasmids were the source hygromycin and nourseothricin resistance cassettes, respectively. Plasmids were maintained in *Escherichia coli* grown at 37 °C in LB broth or on agar supplemented with 50 $\mu g \cdot mL^{-1}$ kanamycin.

In silico analysis of the *C. neoformans PMC1* ortholog

The putative *C. neoformans PMC1* gene sequence was identified by a BLAST search of the *C. neoformans* var. *grubii* strain H99 genomic database at the Broad Institute using the Pmc1 sequence of *S. cerevisiae* (*S. cerevisiae* Genome Database, accession number YGL006W). The amino acid sequences of Pmc1 orthologs from *S. cerevisiae*, *Candida albicans*, *A. fumigatus*, *U. maydis*, *M. oryzae*, *Caenorhabditis elegans* and *C. neoformans* were aligned using CLUSTALX2. Mega4 was utilized for phylogenetic analysis using the neighbor-joining method, and the tree architecture was inferred from bootstrap values obtained from 1000 resamplings. Search for conserved domains in the *C. neoformans* Pmc1 amino acid sequence was performed using the Pfam database (http://pfam.sanger.ac.uk/). The TMHMM server was utilized for prediction of putative transmembrane segments (http://www.cbs.dtu.dk/services/TMHMM/).

Disruption and complementation of *C. neoformans PMC1*

Disruption of *PMC1* was achieved using plasmid constructs generated by the DelsGate method [18]. The 5′ and 3′ *PMC1* flanks (~ 700 bp each) were PCR-amplified and gel-purified using Illustra GFX PCR DNA and Gel Band Purification kit (GE Healthcare, Uppsala, Sweden). Approximately 300 ng of the pDONR-NAT vector [32] and 30 ng of each PCR product were used in the Gateway BP clonase reaction, according to the manufacturer's instructions (Invitrogen). The reaction product was transformed into *E. coli* OmniMAX 2-T1 cells. After confirmation of the correct deletion construct, the plasmid was linearized by I-SceI digestion prior to biolistic *C. neoformans* transformation [33]. Transformants were screened by colony PCR, and the deletion was confirmed by southern blot analysis. For complementation, a 6.6 kb genomic PCR fragment carrying the WT *PMC1* gene and regulatory regions was cloned into the *Eco*RV site of pJAF15 vector. The resulting plasmid was used for transformation of the *pmc1* mutant strain and hygromycin was used to select for positive transformants. Random genomic insertion of the complemented gene was confirmed by southern blot analysis. To construct the *pmc1 vcx1* double mutant, the same plasmid used to construct the *pmc1* mutant strain was used to transform *vcx1* mutant cells. The primers used for these constructions are listed in Table S1.

Phenotypic characterization assays

For phenotypic characterization, WT, mutant (*pmc1*, *vcx1* and *pmc1 vcx1*) and complemented strains were grown on YPD medium for 16 h, washed with $NaCl/P_i$ and adjusted to a cell density of 10^7 cells$\cdot mL^{-1}$ in YPD. The cell suspensions were serially diluted 10-fold, and 3 μL of each dilution was spotted onto YPD agar supplemented with $CaCl_2$ (1, 5, 10, 20, 100, 200, 300, 400 or 500 mM), $MnCl_2$ (4 mM) or $CdCl_2$ (50 μM). The plates were incubated for 2 days at 30 °C and photographed. Melanin production was examined on glucose-free asparagine medium agar plates (1 $g \cdot L^{-1}$ L-asparagine, 0.5 $g \cdot L^{-1}$ $MgSO_4.7H_2O$, 3 $g \cdot L^{-1}$ KH_2PO_4 and 1 $mg \cdot L^{-1}$ thiamine) containing 1 mM L-3,4-dihydroxyphenylalanine [34]. Capsule formation was evaluated in cells that were cultivated for 48 h in DMEM at 37 °C in 5% CO_2 or for 48 h at 30 °C in a minimal medium composed of dextrose (15 mM), $MgSO_4$ (10 mM), KH_2PO_4 (29.4 mM), glycine (13 mM) and thiamine-HCl (3 μM) (pH 5.5). Cell viability was monitored by colony forming unit (CFU) determination. Relative capsule sizes were defined as the distance between the cell wall and the capsule outer border divided by values of cell diameter. IMAGEJ software (http://rsbweb.nih.gov/ij/) was utilized for capsule measurements in at least 50 cells of each strain. Extracellular polysaccharide contents were evaluated by ELISA using antibodies to GXM, as described elsewhere [35]. Cell surface morphology was analyzed after incubation of yeast cells with calcofluor white and the monoclonal antibody 18B7, which recognizes GXM [36]. These probes were used to visualize cell wall chitin (calcofluor) and GXM (18B7) by confocal microscopy following a previously described protocol [37].

Determination of relative intracellular Ca^{2+} levels

The relative intracellular Ca^{2+} concentration was determined using Fura-2 AM according to a previously described protocol [18]. Briefly, WT, *pmc1*, *pmc1 vcx1* and complemented cells were cultured in YPD medium overnight with shaking at 30 °C. Subsequently, 10^7 cells of each strain were incubated for 1 h in fresh YPD supplemented with 100 mM $CaCl_2$. The cells were washed with $NaCl/P_i$ and incubated with 10 μM Fura-2 AM for 30 min at 37 °C. Fura-2 fluorescence was measured at excitation wavelengths of 340 and 380 nm and an emission wavelength of 505 nm. The relative intracellular calcium concentration was expressed as the ratio of fluorescence intensities obtained by excitation at wavelengths of 340 and 380 nm. All data presented are representative of three independent experiments.

Quantitative real-time RT-PCR analysis

For RNA extraction, cultures of WT, *pmc1*, *pmc1 vcx1* and *vcx1* mutant cells were grown overnight in YPD medium at 37 °C with shaking. Subsequently, 10^7 cells of each strain were incubated for 10 min in fresh YPD with or without 100 mM $CaCl_2$. Three independent RNA samples were prepared using TRIzol reagent (Invitrogen) according to the manufacturer's protocol. After DNase treatment, reverse transcriptase reactions were performed. Real-time PCR reactions were performed using StepOne Real-Time PCR System (Applied Biosystems, Foster City, CA, USA). PCR thermal cycling conditions included an initial step at 95 °C for 5 min followed by 40 cycles at 95 °C for 15 s and 60 °C for 1 min. Platinum SYBR green qPCR Supermix (Invitrogen) supplemented with 5 pmol of each primer and 2 μL of the cDNA template in a final volume of 20 μL was used as the reaction mix. Each cDNA sample was analyzed in triplicate with each primer pair. Melting curve analysis was performed at the end of the reaction to confirm the amplification of a single PCR product. Data were normalized to actin cDNA amplified in each set of PCR experiments. The $2^{-\Delta CT}$ method was used to determine the relative expression [38]. The primers utilized in these experiments are listed in Table S1.

Virulence assay

Virulence studies were conducted according to a previously described intranasal inhalation infection model [18] using seven female BALB/c mice (~ 5 weeks old) for each strain. Fungal cells were cultured overnight in 50 mL of YPD medium at 30 °C with shaking, washed twice with $NaCl/P_i$ and suspended in the same buffer. Mice were infected with 10^5 yeast cells suspended in 50 μL $NaCl/P_i$ and monitored daily for survival. The Mantel–Cox test for survival analysis was performed using PRISM GRAPHPAD software. For determination of fungal burden, mice ($n = 4$) were infected as described above. At days 3, 7, 14 and 19 post-infection, the animals were euthanized, and the lungs and brain were aseptically excised. These tissues were macerated in $NaCl/P_i$, and after removal of host cell debris the resulting suspensions were plated on YPD for CFU determination. Student's t test was used to determine the statistical significance of differences in CFU counts. The use of animals in this work was performed with approval of the Universidade Federal do Rio Grande do Sul Ethics Committee for Use of Animals. Mice were housed in groups of four kept in filtered top ventilated cages with food and water *ad libitum*. The animals were cared for according to the Brazilian National Council for Animal Experimentation Control (CONCEA) and Brazilian College of Animal Experimentation (COBEA) guidelines. All efforts to minimize animal suffering were made. Before infection assays, mice were intraperitoneally anesthetized with 100 $mg \cdot kg^{-1}$ ketamine and 16 $mg \cdot kg^{-1}$ xylazine. Mice were analyzed twice daily for any signs of suffering, defined by weight loss, weakness or inability to obtain feed or water. At the first signs of suffering, mice were humanely sacrificed.

Acknowledgements

This work was supported by grants from the Brazilian agencies Conselho Nacional de Desenvolvimento Científico e Tecnológico (CNPq), Coordenação de Aperfeiçoamento de Pessoal de Nível Superior (CAPES) and Fundação de Amparo a Pesquisa no Estado do Rio Grande do Sul (FAPERGS). We thank Joseph Heitman and Alex Idnurm for providing pJAF15 and pAI4 and Arturo Casadevall for providing the monoclonal antibody 18B7. We also thank the Electron Microscopy Center of the Federal University of Rio Grande do Sul (CME, UFRGS) for the confocal microscopy analysis and Henrique Biehl for technical assistance.

References

1 Berridge MJ, Lipp P & Bootman MD (2000) The versatility and universality of calcium signalling. *Nat Rev Mol Cell Biol* **1**, 11–21.
2 Kraus PR & Heitman J (2003) Coping with stress: calmodulin and calcineurin in model and pathogenic fungi. *Biochem Biophys Res Commun* **311**, 1151–1157.
3 Yoshimoto H, Saltsman K, Gasch AP, Li HX, Ogawa N, Botstein D, Brown PO & Cyert MS (2002) Genome-wide analysis of gene expression regulated by the calcineurin/Crz1p signaling pathway in *Saccharomyces cerevisiae*. *J Biol Chem* **277**, 31079–31088.
4 Stathopoulos-Gerontides A, Guo JJ & Cyert MS (1999) Yeast calcineurin regulates nuclear localization of the

Crz1p transcription factor through dephosphorylation. *Genes Dev* **13**, 798–803.
5 Reedy JL, Filler SG & Heitman J (2010) Elucidating the *Candida albicans* calcineurin signaling cascade controlling stress response and virulence. *Fungal Genet Biol* **47**, 107–116.
6 Steinbach WJ, Cramer RA Jr, Perfect BZ, Asfaw YG, Sauer TC, Najvar LK, Kirkpatrick WR, Patterson TF, Benjamin DK Jr, Heitman J *et al.* (2006) Calcineurin controls growth, morphology, and pathogenicity in *Aspergillus fumigatus*. *Eukaryot Cell* **5**, 1091–1103.
7 Odom A, Muir S, Lim E, Toffaletti DL, Perfect J & Heitman J (1997) Calcineurin is required for virulence of *Cryptococcus neoformans*. *EMBO J* **16**, 2576–2589.
8 Chen YL, Lehman VN, Lewit Y, Averette AF & Heitman J (2013) Calcineurin governs thermotolerance and virulence of *Cryptococcus gattii*. *G3 (Bethesda) 3*, **52**, 7–539.
9 Kozubowski L, Lee SC & Heitman J (2009) Signalling pathways in the pathogenesis of *Cryptococcus*. *Cell Microbiol* **11**, 370–380.
10 Kozubowski L, Aboobakar EF, Cardenas ME & Heitman J (2011) Calcineurin colocalizes with P-bodies and stress granules during thermal stress in *Cryptococcus neoformans*. *Eukaryot Cell* **10**, 1396–1402.
11 Kraus PR, Fox DS, Cox GM & Heitman J (2003) The *Cryptococcus neoformans* MAP kinase Mpk1 regulates cell integrity in response to antifungal drugs and loss of calcineurin function. *Mol Microbiol* **48**, 1377–1387.
12 Fox DS, Cruz MC, Sia RA, Ke H, Cox GM, Cardenas ME & Heitman J (2001) Calcineurin regulatory subunit is essential for virulence and mediates interactions with FKBP12-FK506 in *Cryptococcus neoformans*. *Mol Microbiol* **39**, 835–849.
13 Cruz MC, Fox DS & Heitman J (2001) Calcineurin is required for hyphal elongation during mating and haploid fruiting in *Cryptococcus neoformans*. *EMBO J* **20**, 1020–1032.
14 Lev S, Desmarini D, Chayakulkeeree M, Sorrell TC & Djordjevic JT (2012) The Crz1/Sp1 transcription factor of *Cryptococcus neoformans* is activated by calcineurin and regulates cell wall integrity. *PLoS ONE* **7**, e51403.
15 Kraus PR, Nichols CB & Heitman J (2005) Calcium- and calcineurin-independent roles for calmodulin in *Cryptococcus neoformans* morphogenesis and high-temperature growth. *Eukaryot Cell* **4**, 1079–1087.
16 Liu M, Du P, Heinrich G, Cox GM & Gelli A (2006) Cch1 mediates calcium entry in *Cryptococcus neoformans* and is essential in low-calcium environments. *Eukaryot Cell* **5**, 1788–1796.
17 Fan W, Idnurm A, Breger J, Mylonakis E & Heitman J (2007) Eca1, a sarcoplasmic/endoplasmic reticulum Ca^{2+}ATPase, is involved in stress tolerance and virulence in *Cryptococcus neoformans*. *Infect Immun* **75**, 3394–3405.
18 Kmetzsch L, Staats CC, Simon E, Fonseca FL, de Oliveira DL, Sobrino L, Rodrigues J, Leal AL, Nimrichter L, Rodrigues ML *et al.* (2010) The vacuolar Ca^{2+} exchanger Vcx1 is involved in calcineurin-dependent Ca^{2+} tolerance and virulence in *Cryptococcus neoformans*. *Eukaryot Cell* **9**, 1798–1805.
19 Pittman JK (2011) Vacuolar Ca^{2+} uptake. *Cell Calcium* **50**, 139–146.
20 Cunningham KW & Fink GR (1994) Calcineurin-dependent growth control in *Saccharomyces cerevisiae* mutants lacking PMC1, a homolog of plasma membrane Ca^{2+} ATPases. *J Cell Biol* **124**, 351–363.
21 Ma H & May RC (2009) Virulence in *Cryptococcus* species. *Adv Appl Microbiol* **67**, 131–190.
22 Mielniczki-Pereira AA, Hahn AB, Bonatto D, Riger CJ, Eleutherio EC & Henriques JA (2011) New insights into the Ca^{2+}-ATPases that contribute to cadmium tolerance in yeast. *Toxicol Lett* **207**, 104–111.
23 O'Meara TR & Alspaugh JA (2012) The *Cryptococcus neoformans* capsule: a sword and a shield. *Clin Microbiol Rev* **25**, 387–408.
24 Chun CD & Madhani HD (2010) Ctr2 links copper homeostasis to polysaccharide capsule formation and phagocytosis inhibition in the human fungal pathogen *Cryptococcus neoformans*. *PLoS ONE* **5**, e12503.
25 Kmetzsch L, Joffe LS, Staats CC, de Oliveira DL, Fonseca FL, Cordero RJ, Casadevall A, Nimrichter L, Schrank A, Vainstein MH *et al.* (2011) Role for Golgi reassembly and stacking protein (GRASP) in polysaccharide secretion and fungal virulence. *Mol Microbiol* **81**, 206–218.
26 Cunningham KW & Fink GR (1996) Calcineurin inhibits VCX1-dependent H^+/Ca^{2+} exchange and induces Ca^{2+} ATPases in *Saccharomyces cerevisiae*. *Mol Cell Biol* **16**, 2226–2237.
27 Griffiths EJ, Kretschmer M & Kronstad JW (2012) Aimless mutants of *Cryptococcus neoformans*: failure to disseminate. *Fungal Biol Rev* **26**, 61–72.
28 Dinamarco TM, Freitas FZ, Almeida RS, Brown NA, dos Reis TF, Ramalho LN, Savoldi M, Goldman MH, Bertolini MC & Goldman GH (2012) Functional characterization of an *Aspergillus fumigatus* calcium transporter (PmcA) that is essential for fungal infection. *PLoS ONE* **7**, e37591.
29 Nguyen QB, Kadotani N, Kasahara S, Tosa Y, Mayama S & Nakayashiki H (2008) Systematic functional analysis of calcium-signalling proteins in the genome of the rice-blast fungus, *Magnaporthe oryzae*, using a high-throughput RNA-silencing system. *Mol Microbiol* **68**, 1348–1365.
30 Fraser JA, Subaran RL, Nichols CB & Heitman J (2003) Recapitulation of the sexual cycle of the primary fungal pathogen *Cryptococcus neoformans* var. *gattii*:

implications for an outbreak on Vancouver Island Canada. *Eukaryot Cell* **2**, 1036–1045.
31 Idnurm A, Reedy JL, Nussbaum JC & Heitman J (2004) *Cryptococcus neoformans* virulence gene discovery through insertional mutagenesis. *Eukaryot Cell* **3**, 420–429.
32 Schneider Rde O, Fogaca Nde S, Kmetzsch L, Schrank A, Vainstein MH & Staats CC (2012) Zap1 regulates zinc homeostasis and modulates virulence in *Cryptococcus gattii*. *PLoS ONE* **7**, e43773.
33 Toffaletti DL, Rude TH, Johnston SA, Durack DT & Perfect JR (1993) Gene transfer in *Cryptococcus neoformans* by use of biolistic delivery of DNA. *J Bacteriol* **175**, 1405–1411.
34 Baker LG, Specht CA, Donlin MJ & Lodge JK (2007) Chitosan, the deacetylated form of chitin, is necessary for cell wall integrity in *Cryptococcus neoformans*. *Eukaryot Cell* **6**, 855–867.
35 Casadevall A, Mukherjee J & Scharff MD (1992) Monoclonal antibody based ELISAs for cryptococcal polysaccharide. *J Immunol Methods* **154**, 27–35.
36 Casadevall A, Cleare W, Feldmesser M, Glatman-Freedman A, Goldman DL, Kozel TR, Lendvai N, Mukherjee J, Pirofski LA, Rivera J *et al.* (1998) Characterization of a murine monoclonal antibody to *Cryptococcus neoformans* polysaccharide that is a candidate for human therapeutic studies. *Antimicrob Agents Chemother* **42**, 1437–1446.
37 Fonseca FL, Nimrichter L, Cordero RJ, Frases S, Rodrigues J, Goldman DL, Andruszkiewicz R, Milewski S, Travassos LR, Casadevall A *et al.* (2009) Role for chitin and chitooligomers in the capsular architecture of *Cryptococcus neoformans*. *Eukaryot Cell* **8**, 1543–1553.
38 Livak KJ & Schmittgen TD (2001) Analysis of relative gene expression data using real-time quantitative PCR and the 2(-delta delta C(T)) method. *Methods* **25**, 402–408.

Supporting information

Additional supporting information may be found in the online version of this article at the publisher's web site:

Fig. S1. Disruption and complementation of *C. neoformans PMC1*.

Fig. S2. Disruption of *C. neoformans PMC1* does not interfere with melanin production or with the ability to grow at 37 °C.

Fig. S3. The *C. neoformans pmc1 vcx1* mutant displayed sensitivity to 5% CO_2.

Table S1. List of primers used in this study.